Schnagel Lab Rotation - Modeling of Early Fly Olfaction

Always be faking data

Gerick Lee

1 Introduction

Partially inspired by the work of Bell, Sawtell, and their colleagues, I sought to model the early olfactory stages of *Drosophila.* I hypothesized that the onset transient seen in Olfactory Receptor Neurons (ORNs) might be removed by the Local Neurons (LNs) in a manner similar to that seen in the weakly electric fish.

To model this, I used a model of ORNs similar to that in Nagel et al., 2011. Both linear (convolutional) models and dynamical firing rate models were created, and were fed into a delay-line LN model, where increases in the odor strength (not the ORNs) would generate a single firing rate increase after a fixed delay. These firing rates were then fed into a model of the Projection Neurons (PNs), which used a simple anti-Hebbian learning rule to adjust the weights of the inhibitory neurons.

2 Groundwork

As a first step, I needed to generate reliable gaussian filters (the linear ORN models were generated using either a difference-of-gaussians or gaussian-by-line multiplication). Figure 1 shows a test signal ($\boldsymbol{A}$) and the frequency representation of that signal, with an overlapping gaussian filter ($\boldsymbol{B}$). The filter has a Full-Width-at-Half-Max (FWHM) of 2 Hz, which can be seen in the figure.

3 ORN Modelling

For my investigation of PN responses, I first needed a model of ORNs. I began with a linear filter model before moving to a dynamical model, inspired by

Figure 1: **A:** Example signal with non-zero components at the DC, 2Hz, and 3Hz. **B:** Fourier Transform of signal (blue), as well as (amplitude-adjusted) filter (red) with FWHM = 2 Hz.

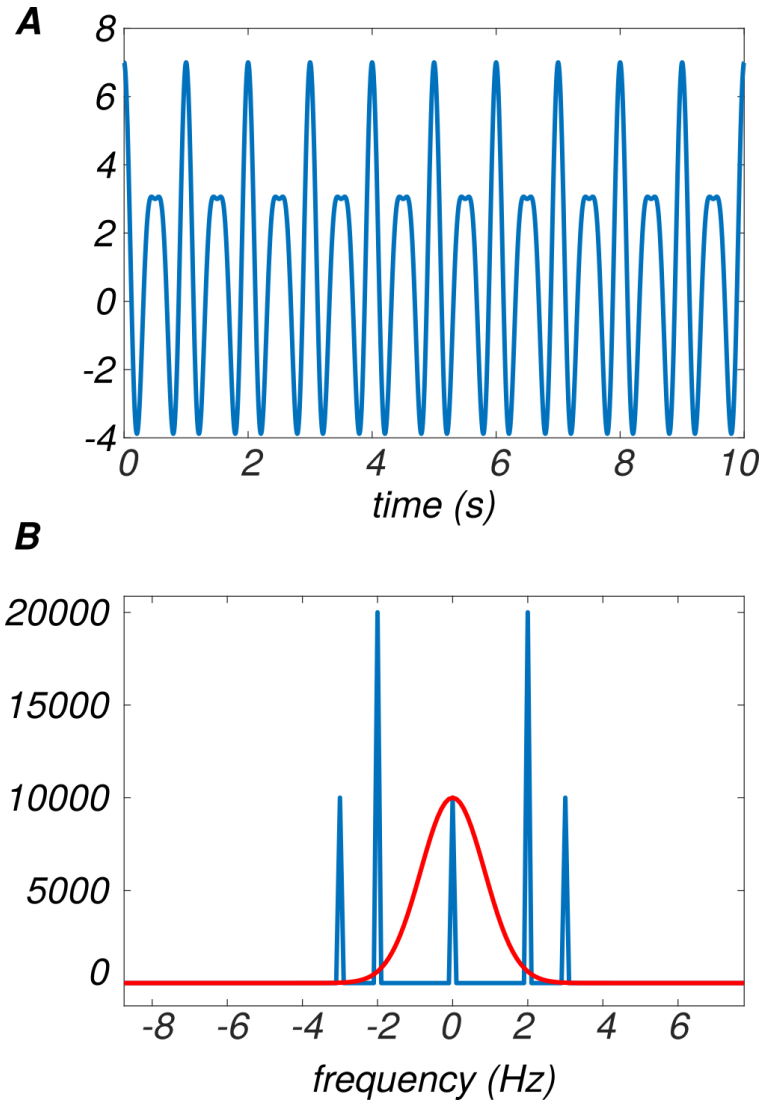

success of the model in Nagel et al., 2011.

3.1 Linear Filter Models

3.1.1 Difference-of-Gaussian Model

To model ORNs, I first used a linear filter model using both Difference-of-Gaussians (DoG) and line-gaussian multiplication as my filters in the frequency domain. My first attempt used a DoG filter with five parameters (governing the width of each gaussian, as well as their offset from the signal, and each other). Figure 2 shows an example curve. Note that it is possible to rectify the response at zero, so as to better capture the asymmetries observed *in vivo*.

Figure 2: **Difference-of-Gaussian based linear filter model** Odor pulse (in arbitrary units) is shown in blue.

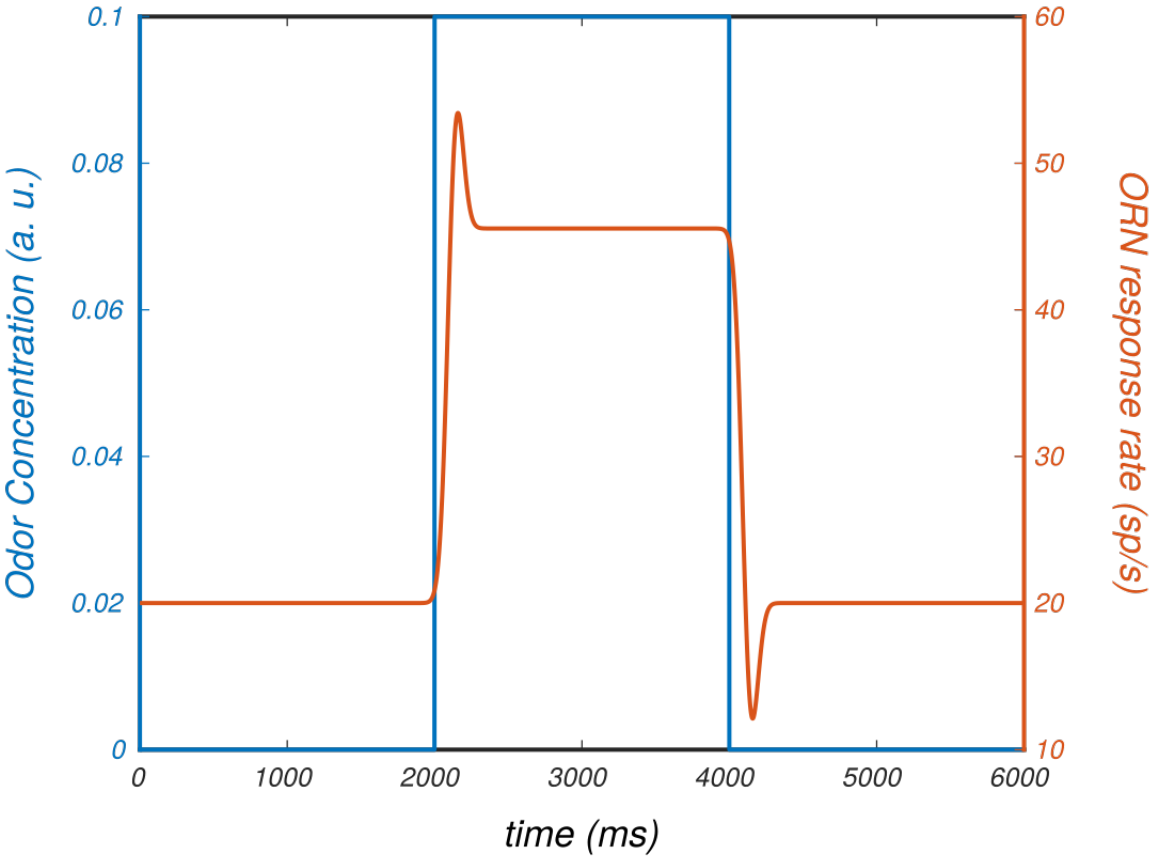

3.1.2 Gaussian-Line Model

To reduce the number of free parameters, I replaced the DoG filter with one multiplying a gaussian filter with a line. This model was also rectified at zero, to avoid negative firing rates (and return more realistic ORN responses). Three example responses (two onset, one offset - all of which were generated using the same function [off and onset are determined by the same parameters]) are shown in Figure 3.

3.2 Dynamic Model

For greater accuracy, I switched to a dynamic model of receptor function. This model was governed by the following:

$$\frac{dR^*}{dt} = k_{on}[O] - (k_{on}[O] + k_{off})R^*, \tag{1}$$

where R^* is the proportion of bound receptor (between 0 and 1), $[O]$ is the odor concentration, and there are two rate constants k. This curve could be multiplied by an arbitrary scalar to better reflect real-world firing rates.

In this model (Figure 4) activation alone varies with concentration (as in Nagel et al., 2011). This model also saturates with increasing concentration (as a result of the limited range of R^*).

Unsatisfied with the shape of the ORN response in this model, I began to experiment with various inactivation terms. I first used a paradigm in which bound receptor (R^*) could vary between an active and inactive (R^i) state (data not shown). I then converged on a model in which inactive receptor recycled back to the unbound state (R). I modelled this with the following equations:

$$\frac{dR^*}{dt} = k_{on}[O] + (k_{re} - k_{on}[O])\, R_i - (k_{on}[O] + k_{off} + k_{de})\, R^*, \tag{2}$$

$$\frac{dR_i}{dt} = k_{de}\, R^* - k_{re}\, R_i, \tag{3}$$

where R_i was the inactive state, k_{de} was the constant of inactivation (from R^* to R_i), and k_{re} was the constant for the conversion from R_i to R.

This model (Figure 5) kept the onset-concentration dependence, and was able to mimic the various shapes of (on response) curves seen in Nagel et al., 2011. These neurons were the ones used for later modelling (if later models require it, offset neurons can be generated using the linear filter model, but none were used for the LN or PN simulations discussed here).

Figure 3: **Variability in ORN firing rates: gaussian-by-line model.** Odor strength (in black, at bottom) is in arbitrary units.

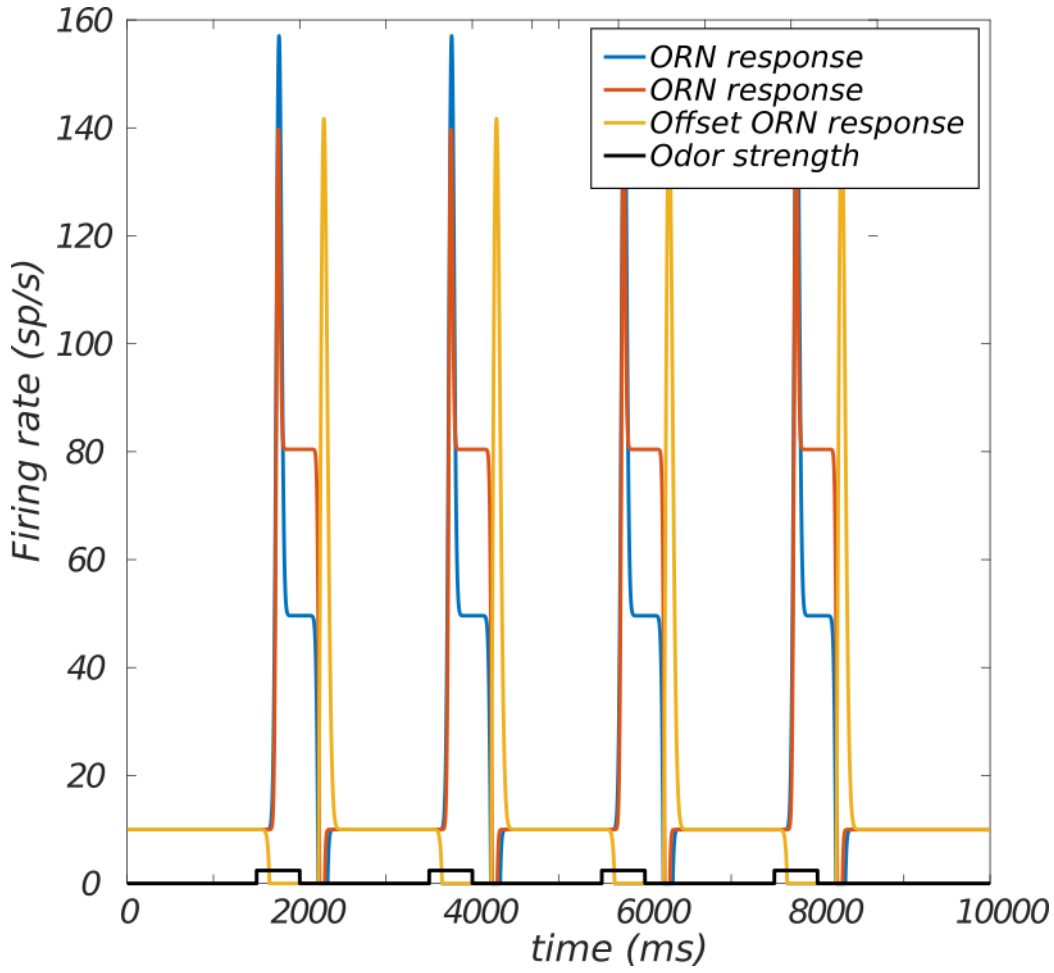

Figure 4: **ORN firing rates: Basic dynamic model.** Odor strength (in black, at bottom) is in arbitrary units, though relative magnitudes are preserved.

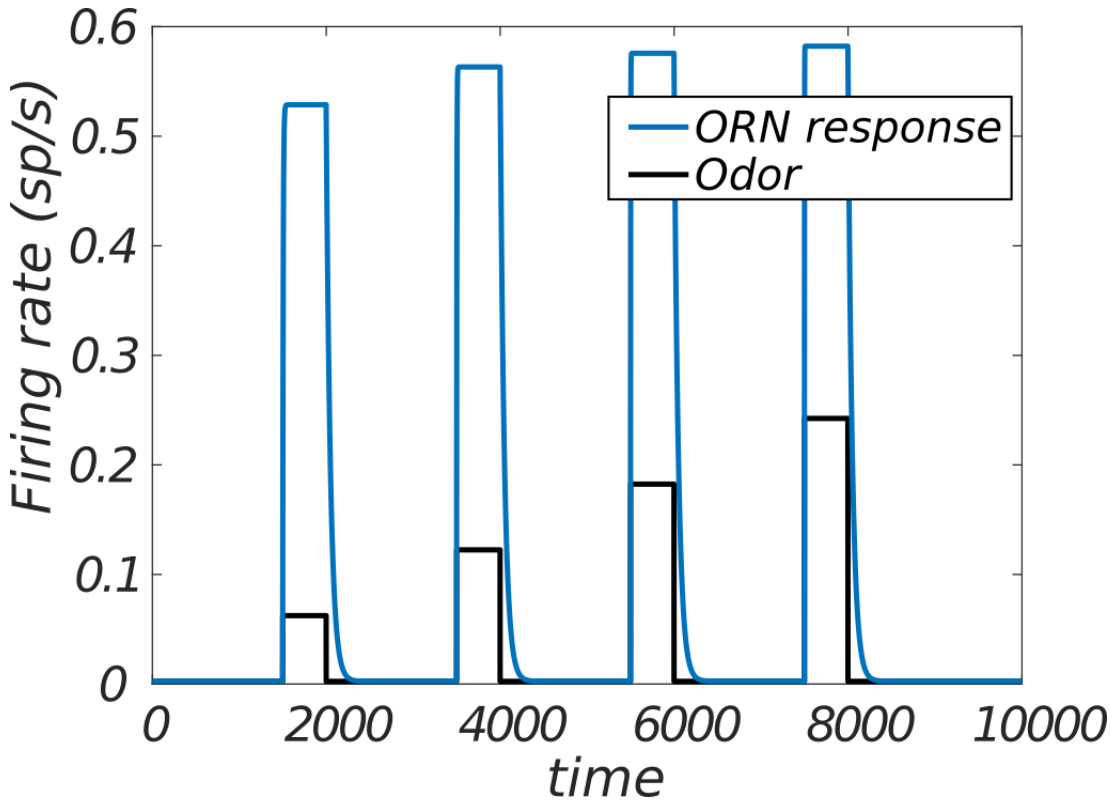

Figure 5: **ORN firing rates: Dynamic model with one-way inactivation.** Odor strength (in black, at bottom) is in arbitrary units.

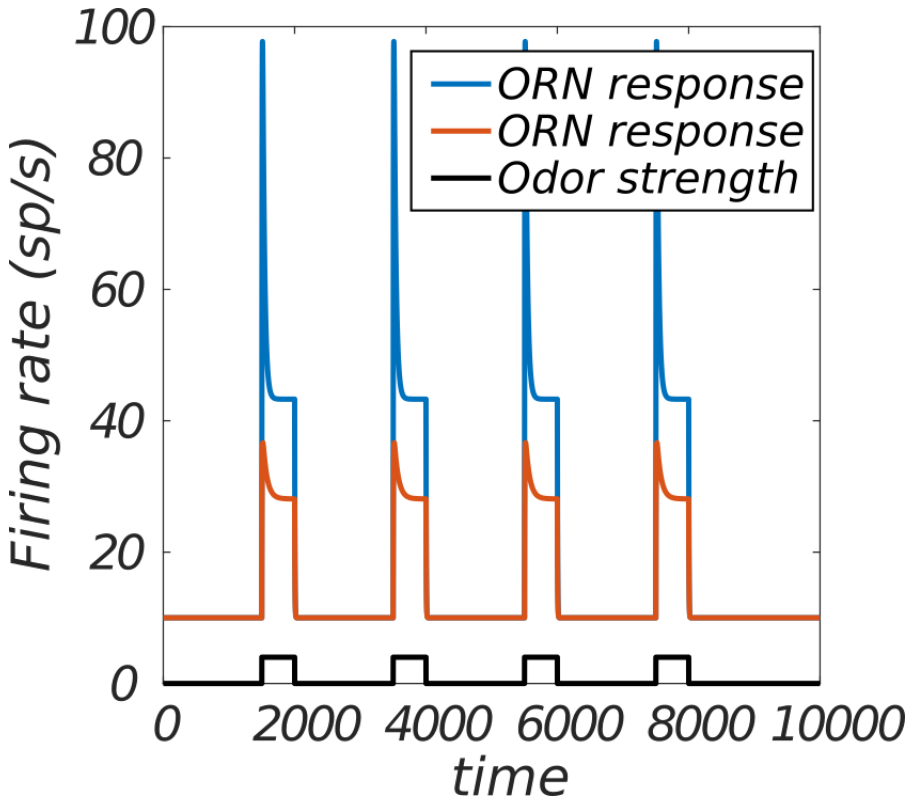

4 LN model

I modelled LNs as a series of delta-like functions, where the odor was used as input. I initially used a simple differentiating linear filter model for my LNs, using ORN outputs as my input. To simplify matters, I shifted to a system where the odor itself was used as the input, and I simply looked for time points where the odor strength had increased since the previous time point (because simulated odors had a clean step shape, this was a trivial operation).

For all increases in odor strength, the LN firing rate would then spike for one time bin, at a fixed delay. Delays were every two time bins for the first 25 of 50 LNs. For the remaining 25, the spacing changed to one every 8 bins (using uniform spacing didn't affect responses in a noticeable way [not shown]). Once initiated by an odor increase, LNs would respond, even if the odor presentation had already ceased. In this model, LN responses are a

time-shifted facisimile of one another. Five example LN responses are shown as Figure 6.

Figure 6: **LN firing rates: Delta function with uniform delay.** Odor strength (in black, at bottom) is in arbitrary units. All LNs are set to the same baseline rate of 0.1 spikes/sec, though it appears as a green line (because the green LN was the last plotted).

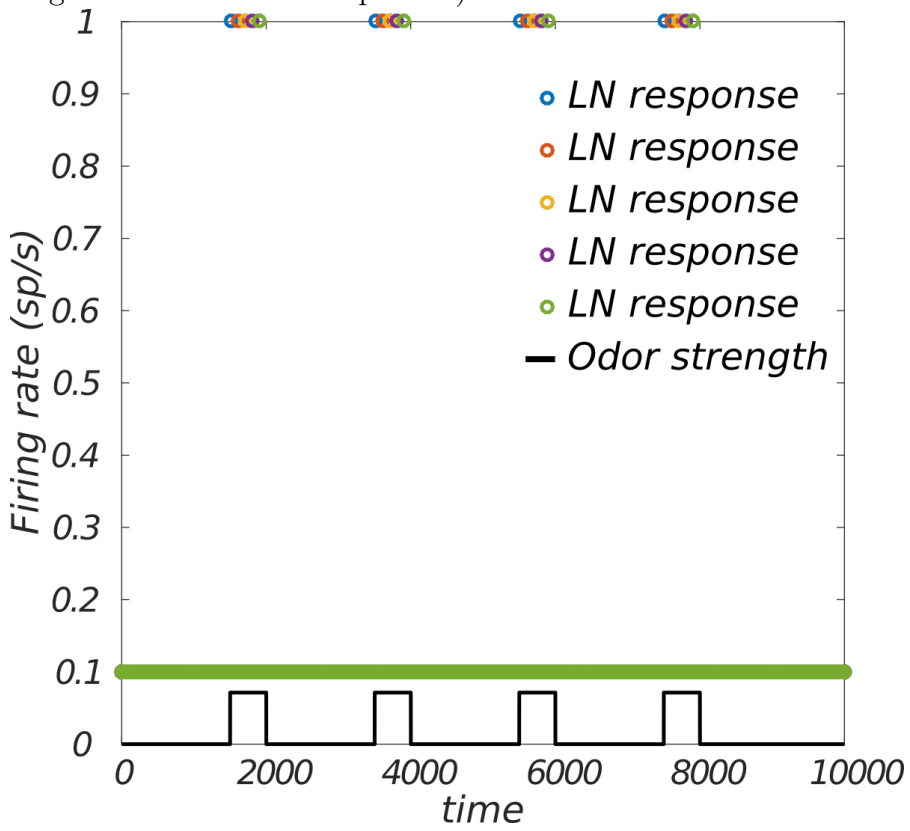

5 PN model

To test whether an anti-Hebbian learning rule could account for behaviors seen in recordings (Nagel et al., 2015), I created a model in which N_{ORN} ORN and N_{LN} LN inputs were merged to generate a firing rate for a single PN. The firing rate r_{PN} was modeled using the Euler method on the following equation:

$$\frac{d\,r_{PN}}{dt} = r_{PN}(t-1) + \sum_{i}^{N_{ORN}} r_{ORN}(t-1) + (\vec{r}_{LN}(t-1) * \vec{w}), \qquad (4)$$

where $r_{ORN}(t)$ is the firing rate of the ORNs (normalized to the global ORN maximum rate), r_{LN} is the LN firing rate, and $\vec{w}$ is the weight vector applied to the LN firing rate. The learning rule used for the weight vector was:

$$\frac{dw}{dt} = \alpha * \Big(r_{LN}(t-1) * \sum_{i}^{N_{ORN}} \big(r_{ORN}(t-1) - \mu_{\vec{r}_{ORN}}(t-\tau : t-1) \big) \Big), \quad (5)$$

where all weights were restricted to the interval $[-1, 0]$. ORN firing rates across τ previous bins were averaged and subtracted from the most recent ORN firing rate (here τ was set to 8). For the first τ timebins, only the $t-1$ value was used.

These ORN rate differences were summed across all ORNs, and this scalar was multiplied by the LN firing rate at time $t-1$. Finally, the resultant value was multiplied by a learning rate α, which was set to -0.1 (the negative sign ensured that weight increases made the LN more negative). Weights were initialized at -0.2.

An example of this PN model is shown as Figure 7. For longer trials (Figure 8) peak responses continue to grow unbounded.

6 Problems

I hoped to demonstrate that LN inhibition could result in a PN response which more faithfully represented the shape of the input odor stimulus. I failed to accomplish this, due to a number of issues. One major issue was the long duration the PN required to return to baseline. Figure 8 demonstrates this - PN responses continue to grow over time, as a result of the long baseline restoration time.

The observed behavior may result from a poor balance of excitation and inhibition. Indeed, by scaling the ORN rate in equation 4 by 0.65, the first few responses more closely resemble the stimulus shape. The ad hoc nature of this solution leaves much to be desired, in any case. A different approach may be to simulate the LN inputs in a more physiologically inspired way, by having LNs synapse presynaptically onto ORNs. This approach might weaken strong ORN transients in a more targeted way, perhaps giving rise to the anticipated (*in vivo*) behavior.

Figure 7: **PN responses** Odor strength (in black, at bottom) is in arbitrary units.

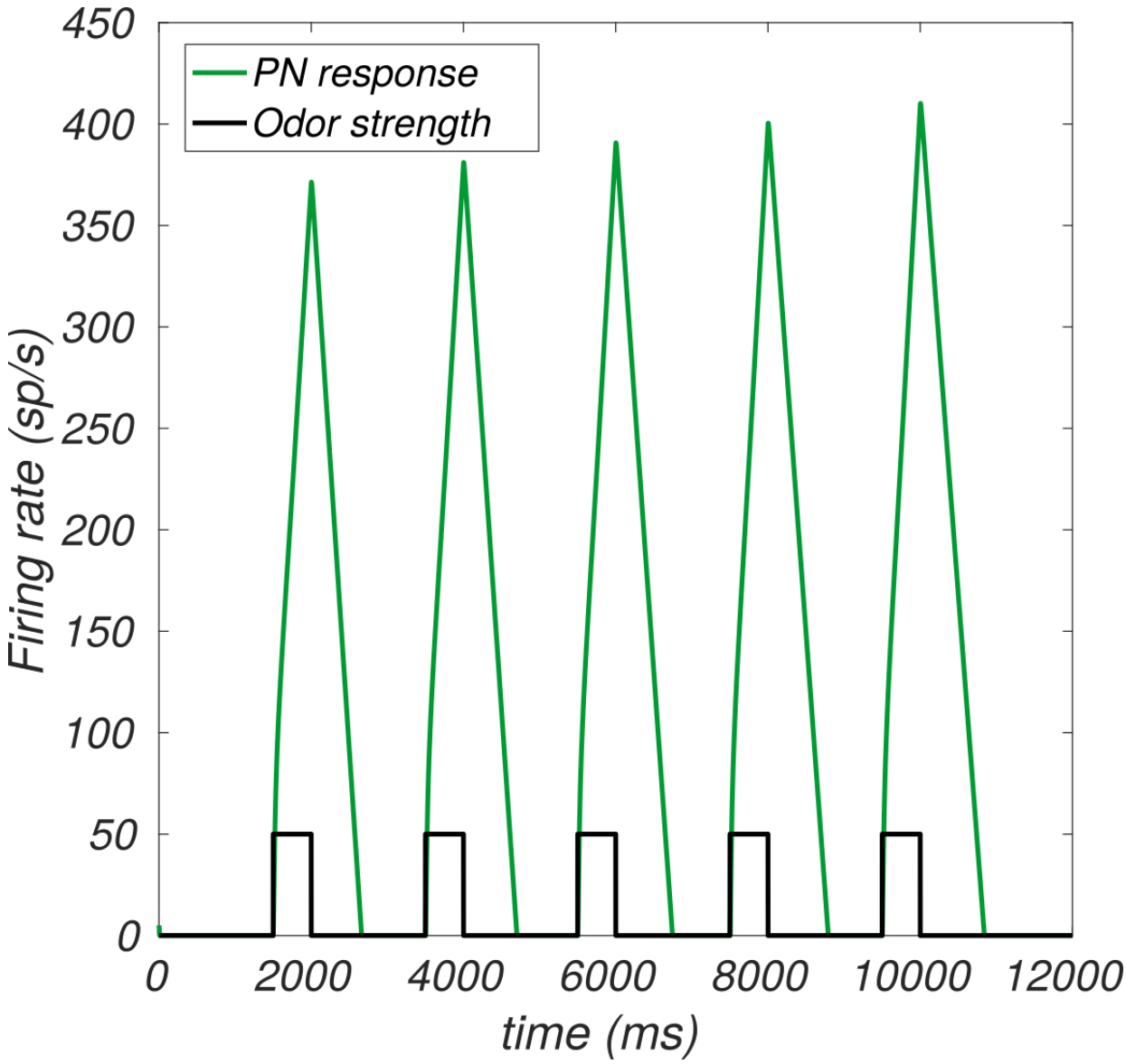

Figure 8: **PN responses with a sustained no-odor period.** Odor strength (in black, at bottom) is in arbitrary units.